



# Removal of Eriochrome Black T Dye by Using Al<sub>2</sub>O<sub>3</sub> Nanoparticles: Central Composite Design, Isotherm and Error Analysis

Ruba Fahmi Abbas<sup>1</sup> · Hawraa Kassem Hami<sup>1</sup> · Neda Ibrahim Mahdi<sup>1</sup> · Ali Amer Waheb<sup>1</sup>

Received: 26 January 2020 / Accepted: 16 June 2020 / Published online: 3 July 2020  
© Shiraz University 2020

## Abstract

Removal of Eriochrome Black T (EBT) dye by using cheap and abundant Al<sub>2</sub>O<sub>3</sub> nanoparticles surface was investigated in this work. Weight of Al<sub>2</sub>O<sub>3</sub> nanoparticles, pH and temperature influence on EBT dye removal was optimized by central composite design coupled with response surface methodology. The obtained removal percentage was in a good agreement with the predicted removal percentage. The minimizing error functions (SAE,  $\chi^2$ , ERRSQ, MPSD and HYBRID) and high value of R<sup>2</sup> were used to find the optimum isotherm model. Based on error functions among two isotherm models enumerated, the Langmuir isotherm model's experimental data gave the present study a better depiction.

**Keywords** Central composite design · Removal · Eriochrome Black T · Al<sub>2</sub>O<sub>3</sub> nanoparticles · SAE

## 1 Introduction

The uses of dyes in industrial fields are one of the most important causes of environmental pollution. These dyes cause toxicity and an effect on living organisms (Yagub et al. 2014; Safa et al. 2014). Eriochrome Black T (EBT) is an azo dye that utilizes in the textile industry, but the presence of this dye in drinking water can be lethal to human health caused by its poisonous and carcinogenic nature, due to its chemically stable structure (Vaiano et al. 2017; Ajitha et al. 2018). The removal of EBT from water is extremely difficult because of its chemical stability and high water solubility (Boudouaia et al. 2019). Many techniques used to get rid of the dye such as photocatalytic (Sharma et al. 2010), oxidation and Fenton process (Bedoui et al. 2009), membrane technology (Hassanzadeh et al. 2017) and

ultrasonic-assisted degradation (Sisi et al. 2020). Compared to other technologies, adsorption technology is easy, environmentally friendly (Chiban et al. 2011), effective and less expensive (Dave et al. 2011).

The continuous development of nanotechnology and its use in removing environmental pollution has increased the interest in using metal oxides nanoparticles as effective surfaces in adsorption technology (Dhawale et al. 2018). Aluminum oxide nanoparticles is an inexpensive surface that has many properties that make it an effective surface in dye removal since it has a high surface area, surface reaction, good absorption capacity, surface acidification and many hydroxide groups (Banerjee et al. 2019).

The study of all adsorption parameters needs to do many experiments and this takes time so we used a central composite designed to reduce the number of practical experiments method and find the interacting influences between the operating factors. Usually, the central composite design (CCD) is used with surface response methodology (RSM) to find optimal conditions and improve the adsorption process (Boudrahem et al. 2019; Garba et al. 2016). Langmuir and Freundlich isotherm conducted to reach the best understanding of potential adsorbent for removal colored dye (Hassani et al. 2015a, b).

The most important points mentioned by the research are:

✉ Ruba Fahmi Abbas  
rubaf1983@uomustansiriyah.edu.iq

Hawraa Kassem Hami  
howraak2012@uomustansiriyah.edu.iq

Neda Ibrahim Mahdi  
nadamahde@uomustansiriyah.edu.iq

Ali Amer Waheb  
alichance80@uomustansiriyah.edu.iq

<sup>1</sup> Department of Chemistry, College of Science, Al-Mustansiriya University, Baghdad, Iraq

- The CCD used to verify the impact of adsorbent dosage, temperature and pH on the adsorption of BET on  $\text{Al}_2\text{O}_3$  nanoparticles
- The appropriate isotherm selected based on the error function values
- Comparing the results with the previous studies

## 2 Materials and Methods

### 2.1 Apparatus

UV–visible spectrophotometer (Cary 100, VARIAN company, USA), pH meter (pH 211, Hanna, USA), XRD (6000, SHIMADZU, Japan) and a shaking water bath (BS-11, lab companion, Korea) were used in this study.

### 2.2 Chemicals

As an adsorbate,  $\text{Al}_2\text{O}_3$  nanoparticles (Hongwu International Group, China) of 99.5% purity and 10–30 nm diameter (shown in Fig. 1) were used. Eriochrome Black T dye has been supplied by BDH. For pH adjustments, 0.01 N HCl (BDH, England) and 0.01 N NaOH (Merck, Germany) were used.

### 2.3 The Experimental Design and Data Analysis

The removal percentage ( $R\%$ ) of experimental values and predicted values were obtained by using a central composite design (CCD) to find the optimum conditions for removal of EBT onto  $\text{Al}_2\text{O}_3$  nanoparticles (Table 1) (Pucarevic et al. 2017).

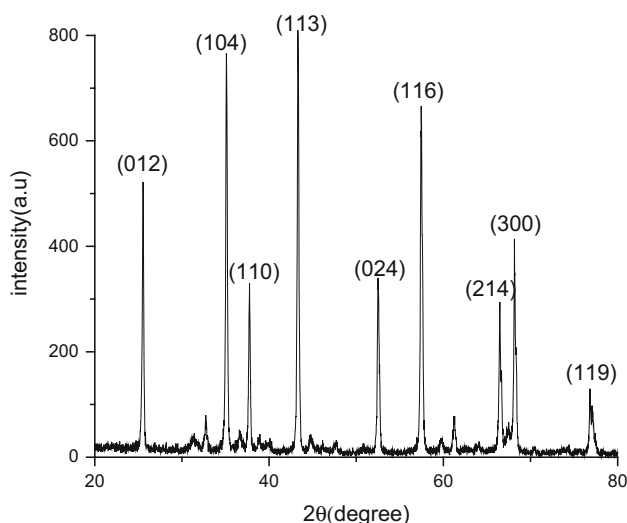


Fig. 1 XRD of standard  $\text{Al}_2\text{O}_3$  nanoparticles

Table 2 shows the levels and range of three important parameters, namely weight of  $\text{Al}_2\text{O}_3$  nanoparticles surface ( $X_1$ ), pH ( $X_2$ ) and temperature ( $X_3$ ) chosen for this study as optimized factors.

Twenty experiments ( $N = 20$ ) were conducted by applying CCD design for three parameters as the following equation:

$$N = 2^3 + (2 \times 3) + 6 = 20 \quad (1)$$

where  $(2 \times 3)$  is axial points,  $2^3$  is factorial points and 6 is central points (Haffad et al. 2019; Ali and Ahmed 2017).

The coded variables are expressed as  $(\pm 1)$  for the factor points,  $(\pm \alpha)$  for the axial points and  $(0)$  for the center points. The test factors are coded as the following (Sivarajasekar et al. 2018):

$$\chi_i = \frac{\alpha[2X_i - (X_{\max} - X_{\min})]}{X_{\max} - X_{\min}} \quad (2)$$

where  $i$  is the  $i$ th variable,  $X_{\max}$  is the highest limits,  $X_{\min}$  is the lowest limits,  $X_i$  is the natural value and finally,  $\chi_i$  is the dimensionless coded value (Table 2) (Khataee et al. 2010).

### 2.4 Adsorption Studies

Adsorption processes using EBT dye have been estimated according to various adsorption factors, such as weight of  $\text{Al}_2\text{O}_3$  nanoparticles, pH and temperature. For this purpose, A weighed of  $\text{Al}_2\text{O}_3$  nanoparticles (0.25 g) were mixed with a 10 mL of (25 mg/L) dye solution in 10mL volumetric flask. Flasks containing the EBT solution and the surface of  $\text{Al}_2\text{O}_3$  nanoparticles were agitated at a constant time 20 min by using a shaking water bath, which was more than enough to achieve equilibrium.

The experiments of isotherm studies were done with four different initial concentrations of dye (25, 35, 45 and 55 mg/L) at different temperatures (35, 45, 55 °C). The final concentration of dye after an adsorption process was determined by using a UV–visible spectrophotometer at 530 nm.

Defined the amount of EBT adsorbed at equilibrium ( $q_e$ ) and its removal percentage ( $R\%$ ) as shown in Eqs. (3) and (4) (Abbas et al. 2019; Hami et al. 2019):

$$q_e = \frac{(C_o - C_e)V}{m} \quad (3)$$

$$R\% = \frac{(C_o - C_e)}{C_o} \times 100 \quad (4)$$

where  $V$  (ml) = volume of EBT,  $C_o$  (mg/L) = initial concentration of EBT,  $m$  (gm) = weight of  $\text{Al}_2\text{O}_3$  nanoparticles surface,  $C_e$  (mg/L) = final concentration of EBT after an adsorption process.

**Table 1** CCD matrix used in the present study

Run	Coded factor			Actual factor			Removal%	
	wt ( $X_1$ )	pH ( $X_2$ )	Temp. ( $X_3$ )	wt ( $X_1$ )	pH ( $X_2$ )	Temp. ( $X_3$ )	Experimental value	Predicted value
1	+ 1	+ 1	+ 1	0.35000	90000	55.000	71.30	70.17
2	+ 1	- 1	- 1	0.35000	2.0000	35.000	85.20	85.72
3	- 1	+ 1	- 1	0.15000	9.0000	35.000	77.20	76.24
4	- 1	- 1	+ 1	0.15000	2.0000	55.000	81.00	82.53
5	0	0	0	0.25000	7.0000	45.000	98.80	92.2
6	0	0	0	0.25000	7.0000	45.000	97.60	92.2
7	+ 1	+ 1	- 1	0.35000	9.0000	35.000	69.40	68.51
8	+ 1	- 1	+ 1	0.35000	2.0000	55.000	76.90	79.8
9	- 1	+ 1	+ 1	0.15000	9.0000	55.000	77.50	76.66
10	- 1	- 1	- 1	0.15000	2.0000	35.000	86.20	88.84
11	0	0	0	0.25000	7.0000	45.000	94.40	92.2
12	0	0	0	0.25000	7.0000	45.000	88.60	92.2
13	- $\alpha$	0	0	0.08183	7.0000	45.000	76.40	80.99
14	+ $\alpha$	0	0	0.41817	7.0000	45.000	87.00	92.34
15	0	- $\alpha$	0	0.25000	1.1141	45.000	65.60	70.01
16	0	+ $\alpha$	0	0.25000	12.8859	45.000	66.60	63.9
17	0	0	- $\alpha$	0.25000	7.0000	28.483	83.40	81.5
18	0	0	+ $\alpha$	0.25000	7.0000	61.517	81.20	82.55
19	0	0	0	0.25000	7.0000	45.000	91.10	92.2
20	0	0	0	0.25000	7.0000	45.000	92.01	92.2

**Table 2** Variables and levels considered for removal EBT

Variables (unit)	- $\alpha$	Low	Center	High	+ $\alpha$
Wt. of surface (mg)	0.081	0.15	0.25	0.35	0.41
pH	1.11	2	7	9	12.88
Temperature (°C)	28.48	35	45	55	61.51

To describe adsorption process properties, Langmuir and Freundlich isotherm models were suggested for this study (Table 3).

### 2.5 Error Function

Five mathematically error functions used in this study are listed in Table 4. The aim to use error functions to measure the goodness-of-fit of isotherm models. In error functions equations,  $n$  (4) = number of experimental data points,  $q_{cal}$ . = calculated EBT dye concentration obtained from isotherm model,  $q_{exp}$ . = experiment dye concentration and  $p$  (2) = number of parameters in each Langmuir and Freundlich isotherm model.

**Table 3** Langmuir and Freundlich isotherm equations

Isotherm	Linear equation	Plot	Parameters	References
Langmuir I	$\frac{C_c}{q_c} = \frac{1}{q_m \cdot KL} + \frac{C_c}{q_m}$	(Ce/qe) versus Ce	$q_m = 1/\text{slope}$ , $KL = \text{slope}/\text{intercept}$	Delil et al. (2019)
Freundlich	$\ln q_e = 1/n \ln C_e + \ln KF$	$\ln q_e$ versus $\ln C_e$	$KF = e^{\text{intercept}}$ , $n = 1/\text{slop}$	Mudzielwana et al. (2019)

**Table 4** Error functions list

Error functions	Equations	References
Sum of the absolute errors function (SAE)	$\sum_{i=1}^n  q_{\text{cal.}} - q_{\text{exp.}} $	Karri et al. (2017)
Chi-square test ( $\chi^2$ )	$\sum_{i=1}^n \frac{(q_{\text{cal.}} - q_{\text{exp.}})^2}{q_{\text{cal.}}}$	Postai et al. (2016)
Sum square error (ERRSQ)	$\sum_{i=1}^n (q_{\text{cal.}} - q_{\text{exp.}})^2$	Demirbas et al. (2008)
Marquardt's percent standard deviation (MPSD)	$100 \sqrt{\frac{1}{n-p} \sum_{i=1}^n \left( \frac{q_{\text{cal.}} - q_{\text{exp.}}}{q_{\text{cal.}}} \right)^2}$	Rostamian and Behnejad (2018)
Hybrid fractional error function (HYBRID)	$\frac{100}{n-p} \sum_{i=1}^n \left[ \frac{(q_{\text{cal.}} - q_{\text{exp.}})^2}{q_{\text{cal.}}} \right]$	Chowdhury et al. (2011)

### 3 Results and Discussion

#### 3.1 XRD Analysis

The crystalline size of the standard gamma  $\text{Al}_2\text{O}_3$  nanoparticles was checked and determined by X-ray meter (Ebrahimia et al. 2019). The conditions of X-ray Diffraction analysis are: scan range = 10–120°,  $\lambda_{\text{Cu}} = 1.5405\text{\AA}$ , tube voltage = 40 (kV), and finally, tube current = 30 (mA).

Debye–Sherrer equation was used to find the means size of  $\text{Al}_2\text{O}_3$  nanoparticles (Hassani et al. 2015a, b):

$$D = \frac{0.9\lambda}{\beta \cos \theta} \quad (5)$$

where  $\lambda = 1.5406$  (X-ray wavelength),  $\beta = \text{FWHM}$  (the line broadening at half of maximum intensity),  $\theta$  = the Bragg angle.

The mean crystalline size of the standard  $\text{Al}_2\text{O}_3$  nanoparticles was obtained 30 nm (Fig. 1).

#### 3.2 Development of Model and Effect of Factors on EBT Removal

Table 1 shows the design matrix containing the factors which effected on the removal of EBT dye on  $\text{Al}_2\text{O}_3$  nanoparticles surface. The optimum conditions to achieve a maximum percentage of dye removal of 98.8 were obtained under the optimum wt of  $\text{Al}_2\text{O}_3$  nanoparticles 0.25, pH of 7 and temperature 45 °C (Fig. 2). The results obtained from Table 1 are evaluated with CCD coupled with RSM for the development of the regression equation for the suggested model's (Agarwal et al. 2016).

The final CCD obtained for percentage removal ( $R\%$ ) of EBT dye by using  $\text{Al}_2\text{O}_3$  nanoparticles surface was suggested by Minitab software and is given as (Dehghani et al. 2018):

$$\begin{aligned} R\% = & -21.0 + 74.6x_1 + 8.71x_2 + 3.20x_3 \\ & - 54.5x_1^2 - 0.7241x_2^2 \\ & - 0.0373x_3^2 - 4.12x_1 \times x_2 - 0.19x_1 \times x_3 \\ & + 0.0424x_2 \times x_3. \end{aligned} \quad (6)$$

From above equation, the individual factors increased EBT dye removal by  $\text{Al}_2\text{O}_3$  nanoparticles surface (positive coefficient values), while the double factors (except  $x_2 \times x_3$ ) decreased dye removal (negative coefficient values) (Garba et al. 2016).

Figure 3 shows the experimental value plotted versus predicted value. In this figure, there are tendencies in the linear regression fit and the fitted regression equation showed a good fit of the CCD model (Gengec et al. 2013).

The ANOVA of EBT removal is listed in Table 5, the  $F$  value of the model is 9.18 and the  $p$  value of the model is 0.001 (less than 0.05) indicating that the CCD model is significant. In this case, the  $p$  values of the ( $x_1$ ), ( $x_2 \times x_2$ ) and ( $x_3 \times x_3$ ) are less than 0.05 on the removal of dye; this means that the EBT removal capacity increases with the increase in these factors and most significant effect, followed by individual factors (pH and temperature). The “ $F$  value of the lack-of-fit” of 1.57 refers to that the lack-of-fit is not significant relative to the pure error. There is 89.21% chance that “ $F$  value of the lack-of-fit” is significant. This large value of  $F$  could be caused by noise. So, it can be concluded that wt of  $\text{Al}_2\text{O}_3$  nanoparticles ( $x_1$ ) play an important role in dye removal (Asfaram et al. 2015; Nekouei et al. 2017).

The high value of regression coefficient  $R^2$  (0.8921 for EBT removal) indicated that 89.21% of the total variation on EBT removal data can be described by the CCD model.

The 3D surface plots easy the determination of the main factors influencing the removal of EBT (Khataee et al. 2010). For the weight of  $\text{Al}_2\text{O}_3$  nanoparticles between (0.15 and 0.35 g) and pH 6 (the temperature is kept constant at 45 °C), 3D-RSM (Fig. 4a) shows the highest dye removal (over 90%).

The adsorption process for removal of EBT onto  $\text{Al}_2\text{O}_3$  nanoparticles was endothermic in nature because of EBT

**Fig. 2** UV–Vis absorption spectrum for removal of 25 mg/L EBT by using Al<sub>2</sub>O<sub>3</sub> nanoparticles at wt of surface 0.25, pH of 7 and temperature 45 °C. The inset shows the photographs taken for (25, 35, 45 and 55 mg/L) EBT before and after adsorption process

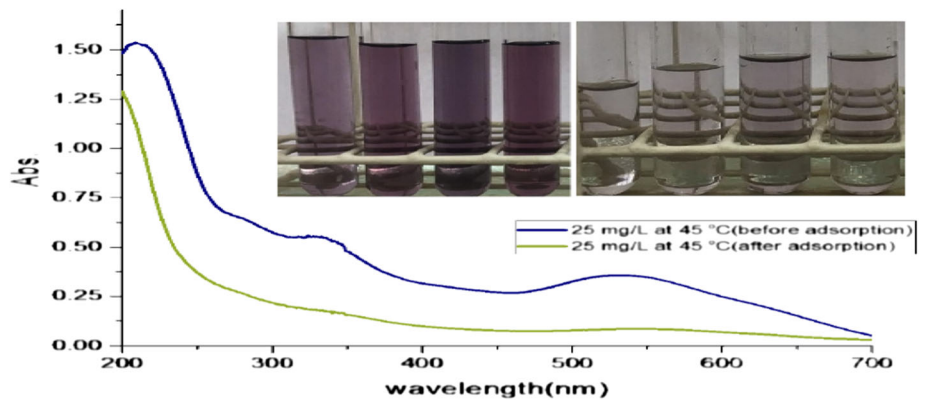


**Fig. 3** Comparisons of the removal% of experimental value plotted versus the predicted values

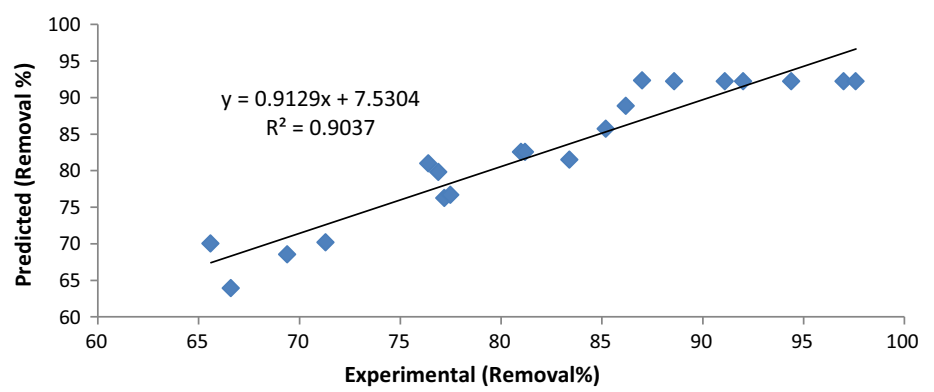


**Table 5** ANOVA for the removal of EBT dye by CCD model

Source	DF (degrees of freedom)	Adj SS (sum of square)	Adj MS (mean of square)	F-Value	P Value
Model	9	1644.76	182.75	9.18	0.001
Linear	3	187.95	62.65	3.15	0.073
X <sub>1</sub>	1	171.83	171.83	8.64	0.015
X <sub>2</sub>	1	31.17	31.17	1.57	0.239
X <sub>3</sub>	1	0.18	0.18	0.01	0.926
Square	3	1398.79	466.26	23.43	0.000
X <sub>1</sub> *X <sub>1</sub>	1	84.87	84.87	4.27	0.066
X <sub>2</sub> *X <sub>2</sub>	1	1216.82	1216.82	61.15	0.000
X <sub>3</sub> *X <sub>3</sub>	1	181.23	181.23	9.11	0.013
2-Way interaction	3	36.24	12.08	0.61	0.625
X <sub>1</sub> *X <sub>2</sub>	1	17.04	17.04	0.86	0.377
X <sub>1</sub> *X <sub>3</sub>	1	0.28	0.28	0.01	0.908
X <sub>2</sub> *X <sub>3</sub>	1	18.92	18.92	0.95	0.353
Error	10	198.98	19.90		
Lack-of-fit	5	121.66	24.33	1.57	0.316
Pure error	5	77.32	15.46		
Total	19	1843.74			

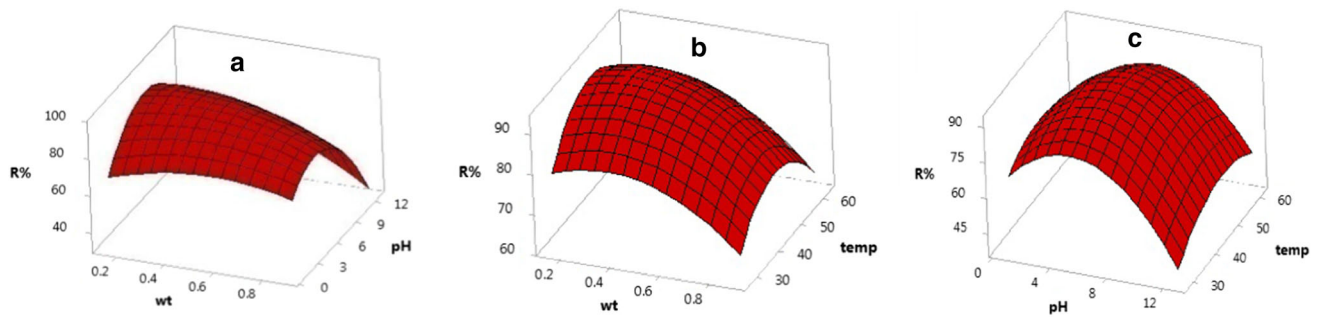
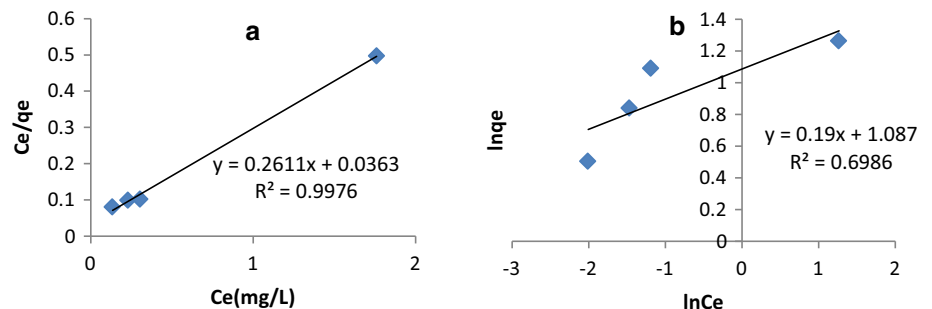


**Fig. 4** 3D surface plots for EBT removal ( $R\%$ ) onto  $\text{Al}_2\text{O}_3$  nanoparticles surface: **a** effect weight of  $\text{Al}_2\text{O}_3$  nanoparticles surface/pH (temperature  $45^\circ\text{C}$ ); **b** effect weight of  $\text{Al}_2\text{O}_3$  nanoparticles surface/temperature (pH 7); **c** effect pH/temperature (weight of  $\text{Al}_2\text{O}_3$  nanoparticles surface 0.15 g)

**Table 6** Linear isotherm constants for adsorption of EBT onto  $\text{Al}_2\text{O}_3$  nanoparticles at  $45^\circ\text{C}$  (wt of surface 0.25 and pH of 7)

Isotherm models	Constants value	SAE	ERRSQ	$X_2$	MPSD	HYBRID	
Langmuir linear	$K_L$	7.25	0.03	0.0009	0.00025	0.39799	0.005633
	$q_m$	3.831					
	$R^2$	0.997					
Freundlich linear	$K_f$	2.965	0.229	0.0524	0.0159	4.8989	0.79503
	$n$	5.263					
	$R^2$	0.698					

**Fig. 5** Linear isotherm for adsorption of EBT onto  $\text{Al}_2\text{O}_3$  nanoparticles at  $45^\circ\text{C}$  (wt of surface 0.25 and pH of 7) **a** Langmuir and **b** Freundlich



removal capacity increased with increasing temperature from  $35$  to  $55^\circ\text{C}$  when the weight of surface 0.25 and pH of 7, as shown in 3D-RSM plots (Fig. 4b, c).

### 3.3 Isotherm Study and Error Functions

Langmuir and Freundlich models were employed for describing the relationship between EBT and  $\text{Al}_2\text{O}_3$  nanoparticles surface at equilibrium (Table 6). The monolayer adsorption of EBT onto the surface of the nanoparticles homogeneous  $\text{Al}_2\text{O}_3$  is called Langmuir isotherm (Ali et al. 2017), while multilayer formation of EBT onto the heterogeneous solid  $\text{Al}_2\text{O}_3$  nanoparticles surface is called Freundlich isotherm. In the Freundlich isotherm model, adsorption capacity ( $n$  and  $k$ ) are Freundlich constants. The weak adsorptive forces are effective on the surface of  $\text{Al}_2\text{O}_3$  nanoparticles when Freundlich

constants have the lower fractional value of  $1/n$  [ $0 < (1/n) < 1$ ] (Khalid and Zubair 2018). The values of five mathematical error functions and regression coefficient ( $R^2$ ) are listed in Table 6. Based on the values of Table 6, it seems that the high value of ( $R^2$ ) for the Langmuir model makes it more adequate to adjusting the adsorption isotherms of EBT dye onto  $\text{Al}_2\text{O}_3$  nanoparticles. A similar result may be observed from the values used in this study for the five error functions. The error functions show that all values are minimum for Langmuir rather than Freundlich, indicating that Langmuir is the best model for this study. The monolayer adsorption capacity ( $q_m$ ) of treated  $\text{Al}_2\text{O}_3$  nanoparticles is found to be  $3.831\text{ mg/g}$ . This means that commercially available and inexpensive  $\text{Al}_2\text{O}_3$  nanoparticles can be used as an adsorbent for the removal of EBT dye from its aqueous solution (Fig. 5).



**Table 7** Comparison of removal percentage ( $R\%$ ) with other adsorbents in the literature

Adsorbent	$R\%$	References
Waste rice hulls (activated carbon)	95.91	de Luna et al. (2013)
Waste activated sludge	97.08	Aly-Eldeen et al. (2018)
HMBL ( $H_3PO_4$ -modified berry leaves)	92	Ahmaruzzaman et al. (2015)
$MnO_2$ -coated zeolite	79.24	Aguila and Ligaray (2015)
$Al_2O_3$ nanoparticles	89.21	Present study

### 3.4 Comparison with Other Studies

The comparison of the removal percentage ( $R\%$ ) of EBT onto different adsorbents surfaces is listed in Table 7. It shows that this work has larger  $R\%$  than those mentioned in previous studies.

## 4 Conclusions

In this study, removal of EBT was achieved by using  $Al_2O_3$  nanoparticles as a cheap and commercially available surface. The effect of the weight of  $Al_2O_3$  nanoparticles, pH and temperature were investigated by using CCD coupled with RSM. The Minitab software showed that the optimum removal of 89.21% was obtained at wt of  $Al_2O_3$  nanoparticles, pH and temperature of 0.25 g, 7 and 45 °C, respectively. The results of  $R^2$  and error functions showed that the Langmuir isotherm was the best-fitted isotherm model.

**Acknowledgements** We thank university of Mustansiriya, College of Science, Department of Chemistry for helpful about doing this work.

## References

- Abbas RF, Hami HK, Mahdi NI (2019) Removal of doxycycline hyclate by adsorption onto cobalt oxide at three different temperatures: isotherm, thermodynamic and error analysis. *Int J Environ Sci Technol* 10:5439–5446
- Agarwal M, Patel D, Dinker A (2016) Optimization of manganese removal from water using response surface methodology. *Iran J Sci Technol Trans A Sci* 40:63–73
- Aguila DM, Ligaray MV (2015) Adsorption of eriochrome black T on  $MnO_2$ -coated zeolite. *Int J Environ Sci Dev* 6:824
- Ahmaruzzaman M, Ahmed MJ, Begum S (2015) Remediation of Eriochrome Black T-contaminated aqueous solutions utilizing  $H_3PO_4$ -modified berry leaves as a non-conventional adsorbent. *Desalin Water Treat* 56:1507–1519
- Ajitha Rani R, Patil MG, Gupta MA (2018) Adsorption of Eriochrome Black T on fly ash: simple and reliable method. *Int J Res Anal Rev* 5:605–611
- Ali MM, Ahmed MJ (2017) Adsorption behavior of doxycycline antibiotic on NaY zeolite from wheat (*Triticum aestivum*) straws ash. *J Taiwan Inst Chem Eng* 81:218–224
- Aly-Eldeen MA, El-Sayed AA, Salem DM, El Zokm GM (2018) The uptake of Eriochrome Black T dye from aqueous solutions utilizing waste activated sludge: adsorption process optimization using factorial design. *Egypt J Aquat Res* 44:179–186
- Asfaram A, Ghaedi M, Agarwal S, Inderjeet Tyagi I, Gupta VK (2015) Removal of basic dye Auramine-O by ZnS: Cu nanoparticles loaded on activated carbon: optimization of parameters using response surface methodology with central composite design. *RSC Adv* 5:18438–18450
- Banerjee S, Dubey S, Gautam RK, Chattopadhyaya MC, Sharma YC (2019) Adsorption characteristics of alumina nanoparticles for the removal of hazardous dye, Orange G from aqueous solutions. *Arab J Chem* 12:5339–5355
- Bedoui A, Ahmadi MF, Bensalah N, Gadri A (2009) Comparative study of Eriochrome black T treatment by BDD-anodic oxidation and Fenton process. *Chem Eng J* 146:98–104
- Boudouaia N, Bengharez B, Jellali S (2019) Preparation and characterization of chitosan extracted from shrimp shells waste and chitosan film: application for Eriochrome black T removal from aqueous solutions. *Appl Water Sci* 9:91
- Boudrahem F, Ziani S, Aissani-Benissad F (2019) Application of response surface methodology based on central composite design for optimization of yellow bezacryl sorption on shoe soles waste. *Environ Prog Sustain Energy* 38:S412–S421
- Chiban M, Soudani A, Fouad Sinan F, Persin M (2011) Single, binary and multi-component adsorption of some anions and heavy metals on environmentally friendly *Carpobrotus edulis* plant. *Colloids Surf B* 82:267–276
- Chowdhury S, Misra R, Kushwaha P, Das P (2011) Optimum sorption isotherm by linear and nonlinear methods for safranin onto alkali-treated rice husk. *Bioremediat J* 15:77–89
- Dave PN, Kaur S, Khosla E (2011) Removal of Eriochrome black-T by adsorption on to eucalyptus bark using green technology. *Indian J Chem Technol* 18:53–60
- De Luna MD, Flores ED, Genuino DA, Futralan CM, Wan MW (2013) Adsorption of Eriochrome Black T (EBT) dye using activated carbon prepared from waste rice hulls—optimization, isotherm and kinetic studies. *J Taiwan Inst Chem Eng* 44:646–653
- Dehghani MH, Pourshabanian M, Heidarinejad Z (2018) Experimental data on the adsorption of Reactive Red 198 from aqueous solution using  $Fe_3O_4$  nanoparticles: Optimization by response surface methodology with central composite design. *Data Brief* 19:2126–2132
- Delil AD, Gülçiçek O, Gören N (2019) Optimization of adsorption for the removal of cadmium from aqueous solution using Turkish coffee grounds. *Int J Environ Res* 13:861–878
- Demirbas E, Kobya MK, Konukman AE (2008) Error analysis of equilibrium studies for the almond shell activated carbon adsorption of Cr(VI) from aqueous solutions. *J Hazard Mater* 154:787–794
- Dhawale VP, Khobragade VB, Kulkarni SD (2018) Synthesis and characterization of aluminium oxide ( $Al_2O_3$ ) nanoparticles and its application in azo dye decolourisation. *Int J Environ Chem* 2:10–17
- Ebrahimia M, Mobasherpour I, Bafrooei HB, Bidabadi FS, Mansoorianfar M, Oroojia Y, Khataeae A, Meia C, Salahi E, Ebadzadeh T (2019) Taguchi design for optimization of structural and

- mechanical properties of hydroxyapatite-alumina-titanium nanocomposite. *Ceram Int* 45:10097–10105
- Garba ZN, Bello I, Galadima A, Lawal AY (2016) Optimization of adsorption conditions using central composite design for the removal of copper (II) and lead (II) by defatted papaya seed. *Karbala Int J Mod Sci.* 2:20–28
- Gengec E, Ozdemir U, Ozbay B, Ozbay I, Veli S (2013) Optimizing dye adsorption onto a waste-derived (modified charcoal ash) adsorbent using Box–Behnken and central composite design procedures. *Water Air Soil Pollut* 224:1751
- Haffad H, Zbair M, Anfar Z, Ahsaine HA, Bouhlal H, Khallok H (2019) Removal of reactive red-198 dye using chitosan as an adsorbent: optimization by Central composite design coupled with response surface methodology. *Toxin Rev* 38:1–13
- Hami HK, Abbas RF, Abed MA, Maryoosh AA (2019) Kinetics study of Removal Doxycycline drug from aqueous solution using Aluminum Oxide surface. *Egypt J Chem* 62:1713–1723
- Hassani A, Kiransan M, Soltani RD, Khataee A, Karaca S (2015a) Optimization of the adsorption of a textile dye onto nanoclay using a central composite design. *Turk J Chem* 39:734–749
- Hassani A, Soltani RDC, Karaca S, Khataee A (2015b) Preparation of montmorillonite–alginate nanobiocomposite for 3 adsorption of a textile dye in aqueous phase: isotherm, kinetic and experimental design approaches. *J Ind Eng Chem* 21:1197–1207
- Hassanzadeh E, Farhadian M, Razmjou A, Askari N (2017) An efficient wastewater treatment approach for a realwoolen textile industry using a chemical assisted NFmembrane process. *Environ Nanotechnol Monit Manag* 8:92–96
- Karri RR, Sahu JN, Jayakumar NS (2017) Optimal isotherm parameters for phenol adsorption from aqueous solutions onto coconut shell based activated carbon: error analysis of linear and non-linear methods. *J Taiwan Inst Chem Eng* 80:472–487
- Khalid A, Zubair M (2018) A comparative study on the adsorption of Eriochrome Black T dye from aqueous solution on graphene and acid-modified graphene. *Arab J Sci Eng* 43:2167–2179
- Khataee AR, Fathinia M, Aber S, Zarei M (2010) Optimization of photocatalytic treatment of dye solution on supported TiO<sub>2</sub> nanoparticles by central composite design: intermediates identification. *J Hazard Mater* 181:886–897
- Mudzielwana R, Gitari MW, Ndungu P (2019) Performance evaluation of surfactant modified kaolin clay in As (III) and As (V) adsorption from groundwater: adsorption kinetics, isotherms and thermodynamics. *Heliyon* 5(11):e02756
- Nekouei F, Kargarzadeh H, Nekouei S, Keshtpour F, Makhlof AH (2017) Efficient method for determination of methylene blue dye in water samples based on a combined dispersive solid phase and cloud point extraction using Cu(OH)<sub>2</sub> nanoflakes: central composite design optimization. *Anal Bioanal Chem* 409:1079–1092
- Postai DL, Demarchi CA, Zanatta F, Melo DC, Rodrigues CA (2016) Adsorption of rhodamine B and methylene blue dyes using waste of seeds of *Aleurites Moluccana*, a low cost adsorbent. *Alex Eng J* 55:1713–1723
- Pucarevic M, Stojic N, Kuzmanovski I (2017) Removal of pesticides from water using zeolites. *Kuwait J Sci* 44:99–105
- Rostamian R, Behnejad H (2018) Insights into doxycycline adsorption onto graphene nanosheet: a combined quantum mechanics, thermodynamics, and kinetic study. *Environ Sci Pollut Res* 25:2528–2537
- Safa Y (2014) Biosorption of Eriochrome Black T and Astrazon FGGL blue using almond and cotton seed oil cake biomass in a batch mode. *J Chem Soc Pak* 36:614–623
- Sharma SU, Chaturvedi NI, Chaturvedi RK, Sharma MK (2010) Photocatalytic degradation of eriochrome black T using ammonium phosphomolybdate semiconductor. *Int J Chem Sci* 8:1580–1590
- Sisi AJ, Khataee A, Fathinia M, Vahid B (2020) Ultrasonic-assisted degradation of a triarylmethane dye using combined peroxydisulfate and MOF-2 catalyst: synergistic effect and role of oxidative species. *J Mol Liq* 297:111838
- Sivarajasekar N, Mohanraj N, Sivamani S, PrakashMaran J, GaneshMoorthy I, Balasubramani K (2018) Statistical optimization studies on adsorption of ibuprofen onto Albizialebeck seed pods activated carbon prepared using microwave irradiation. *Mater Today Proc.* 5:7264–7274
- Vaiano V, Matarangolo M, Sacco O, Sannino D (2017) Photocatalytic Removal of Eriochrome Black T dye over ZnO nanoparticles doped with Pr, Ce or Eu. *Chem Eng Trans* 57:625–630
- Yagub MT, Sen TK, Afroze S, Ang HM (2014) Dye and its removal from aqueous solution by adsorption: a review. *Adv Coll Interface Sci* 209:172–184